The effect of the structure on the physical properties in $Ge_xAs_{10}Se_{90-x}$ glasses

S. W. Xu*, T. W. Liang, X, Y, Zhu
College of Mathematics and Physics, Hunan University of Arts and Science, 415000, Changde, People's Republic of China

We have prepared a group of $Ge_xAs_{10}Se_{90-x}$ glass(x=5, 10, 15, 20, 25, 30, and 35 at. %) and investigated their structure and physical properties. It was found that, the minimum refractive index and maximum optical bandgap occur in $Ge_{25}As_{10}Se_{65}$ glass that is chemically stoichiometric. Analysis of Raman spectra of the glasses indicated that the number of the Ge-Ge, As-As, and Se-Se homopolar bonds is closely related to the bandgap, because the band-tails formed by homopolar bonds could reduce the optical bandgap. The transition behavior of the structural units and physical properties of the glasses occurs at the glass with the chemically stoichiometric composition, and thus the chemical composition dominates physical properties of $Ge_xAs_{10}Se_{90-x}$ chalcogenide glasses.

(Received October 17, 2022; Accepted January 13, 2023)

Keywords: Chalcogenide glasses, Raman spectra, Refractive index, Optical bandgap, Homopolar bond

1. Introduction

Chalcogenide glasses are the combination of chalcogen elements (S, Se and Te) with other metallic or non-metallic elements (Ga, Ge, As, Sb, Si and P, etc.) in the form of the covalent bonds. Because of their extremely high third-order nonlinear coefficient and extremely wide infrared transmittance range [1-5], they can be used in the infrared photonic device such as optical fiber and the waveguide for the applications in the generation of super continuous spectrum, infrared frequency comb, middle infrared Raman fiber laser, and all-optical switch. etc. [6-12]. Many chalcogenide glass systems have large glass forming regions and their physical properties can be easily adjusted by glass compositions. Since the properties of materials are closely related to their microstructure, understanding the change of microstructure with composition of chalcogenide glass is helpful to search for glass with the best properties for the applications in the optical devices.

After decades of continuous research, two models have been suggested to explain the influence of chalcogenide glass composition on the physical properties. The first is the topological model proposed by Phillips based on constraints theory. This model emphasizes that the physical properties of glass are mainly controlled by its mean coordination number (MCN), where, the MCN is defined as the sum of the product of the coordination number of various atoms constituting the covalent glass and their respective percentage concentrations [13]. Thrope pointed out that when MCN<2.4, the covalent network structure inside the glass is loose and less restricted. When MCN>2.4, the restriction degree is too high and the condition is tight. Therefore, the glass structure is the most stable at MCN=2.4 [14]. Tanaka found that when MCN=2.67, there is another structural phase transition in the glass network. When MCN<2.67, the glass structure is in a two-dimensional state, however, when MCN>2.67, the glass structure becomes a three-dimensional state [15]. The second model is the chemical order glass network structure model based on covalent bonds, which holds that most of the glass network structures exist in the form of heteropolar bonds, thus maintaining the chemical order state. Therefore, the structure and physical properties of glass are mainly controlled by its chemical composition [16].

* Corresponding author: xusiwei1227@163.com
https://doi.org/10.15251/CL.2023.201.55

Although these two models can partially explain many problems of chalcogenide glass, there is still no accepted model of glass structure that is both rigorous and complete. This is mainly due to the lack of long-range order in the glasses. Therefore, MCN is still controversial in explaining the variation of the physical properties of ternary glass systems. In recent years, Wang et al studied the thermodynamic properties of Ge-As-Se glasses, they found that the transition activation energy and the transition point of brittleness appeared near MCN= 2.4, while there was no transition feature near MCN=2.67 [17]. Yang et al. studied the relationship between the optical bandgap (E_g) of Ge-As-S chalcogenide glass and the chemical composition of the glass. The results show that the change of the E_g is mainly related to the amount of S content in the glass composition, but not to the MCN [18]. In order to distinguish the different effects of chemical composition and MCN on glass structure and physical properties, a group of $Ge_xAs_{10}Se_{90-x}$ glasses with fixed As content of 10 at. % were prepared in this study. Their refractive index optical band gap and Raman spectra were measured, and then the effects of chemical composition and MCN on their physical properties were analyzed.

2. Experimental

Chalcogenide glasses ($Ge_xAs_{10}Se_{90-x}$) were prepared by melt-quenching technique. The preparation process is as follows: firstly, high purity (5N) Ge, As and Se elemental materials are weighed (20g) according to their chemical composition. Then it was placed in the pre-cleaned quartz ampoule (soaked in the aqua rega for 2~3 h, then take it out and rinsed repeatedly with deionized water and anhydrous ethanol, and placed in the drying oven at 180℃ after drying), and the quartz ampoule was evacuated (the vacuum degree was below 10^{-4} Pa). After that, the quartz ampoule was sealed by oxygen hydrogen torch and placed in a rocking furnace to melt (heating up to 850℃, melting time is more than 20 h). Finally, it was quenched by water cooling method, and annealed by annealing furnace(the annealing temperature was 20℃ below the glass transition temperature T_g for about 3 h).

The refractive indexes of glasses were measured by Metricon Model 2010 prism coupler. The measurement accuracy is ±0.001, and the laser light source is 1550 nm. The wavelength range of the absorption spectrum is 400~1500 nm and the absorption coefficient α is obtained from Formula (1).

$$I(x) = I_0 exp(-\alpha x) \tag{1}$$

where I and I_0 are the intensity of emergent light and intensity of incident light, and x is the distance of light propagation. Then, the Tauc equation is used to calculate the E_g of each glass. The formula is shown in (2) [19]:

$$\alpha h\nu = B(h\nu - E_g)^m \tag{2}$$

where, α, E_g, $h\nu$ and m are the absorption coefficient, optical band gap, photon energy of incident light and type of electron transition, respectively. The B is the constant associated with the band tail.

Raman spectra of glasses were recorded using a micro-Raman spectrometer (Jobin-Yvon-Horiba T64000). In order to avoid the photo-induced effects, we choose 830 nm laser line as the excitation source, and maintain the laser power as small as possible. The Bose-Einstein thermal distribution formula was used to eliminate the influence of thermal effect on Raman spectra, as shown in (3) [20]:

$$I_{red}(\omega) = \frac{\omega}{n+1} \times \frac{1}{(\omega_0 - \omega)^4} \times I_{mea}(\omega) \tag{3}$$

where, ω is Raman frequency, ω_0 is absolute frequency of excitation light source, $I_{mea}(\omega)$ is Raman

intensity of the measurement, and $I_{red}(\omega)$ is Raman intensity after deducting the thermal effect, n is the Bose-Einstein factor, which is formulated as follows (4):

$$n = (exp\ (\hbar\omega/k_B T) - 1)^{-1} \quad (4)$$

where, the h and k_B are Planck's and Boltzmann's constant, respectively. The T is the temperature at the time of measuring Raman spectra. We used PeakFit software to decompose the Raman spectra, and obtained the relevant information (such as position of peak center, full width at half maximum and intensity) of each Raman vibration peak through iterative simulation method.

3. Results and discussion

The refractive index of glass at 1.55 μm wavelength varies with Ge content and MCN, as shown in Fig. 1. The results show that the refractive index of glass decreases initially and then increases according to the chemical composition or MCN of the glass. The minimum value of the refractive index was found at $Ge_{25}As_{10}Se_{65}$, which is chemically stoichiometric, and the corresponding MCN is MCN=2.60. No transition at MCN=2.40 and 2.67 can be observed. It can be preliminarily concluded that the chemical composition of glass plays a major role in affecting the refractive index of glass.

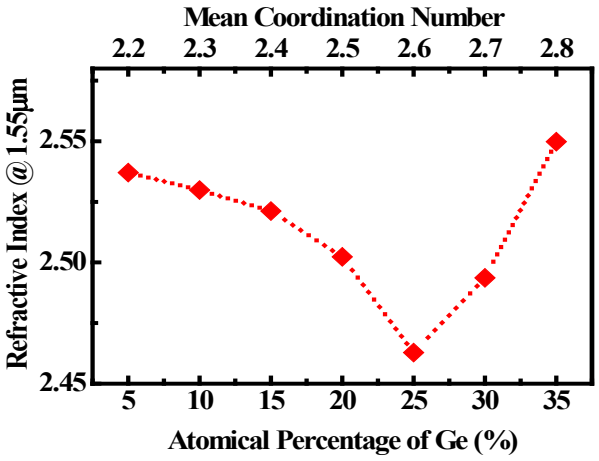

Fig. 1. Variation of the refractive index as a function of the MCN and Ge concentration in $Ge_xAs_{10}Se_{90-x}$ glasses.

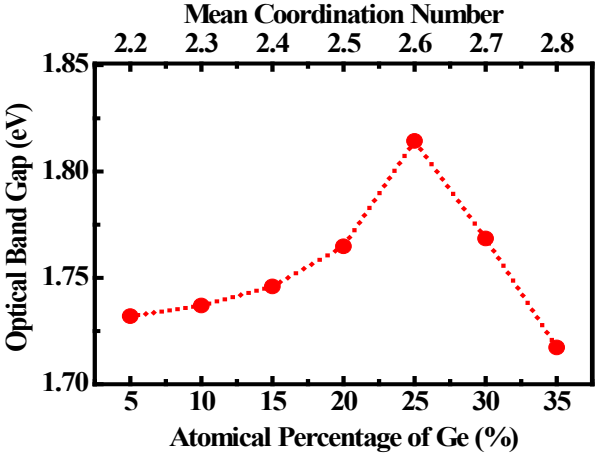

Fig. 2. Variation of the E_g as a function of the MCN and Ge concentration in $Ge_xAs_{10}Se_{90-x}$ glasses.

Fig. 2 shows the variation trend of E_g with chemical composition and MCN. It can be seen that with the increase of Ge content, the E_g increases and then decreases, and the maximum value corresponds to the glass of $Ge_{25}As_{10}Se_{65}$ (MCN=2.60), which indicates that the E_g of glass is mainly affected by its chemical composition as well.

For chalcogenide glasses Ge_xSe_{1-x}, the characteristic peak of Se rings or chains structure appears near 253 cm^{-1} [21-23]. With the increase of Ge concentration, the Raman characteristic peak caused by the vibration mode of corner-sharing (CS) of the $GeSe_{4/2}$ tetrahedral appears near 195 cm^{-1}, and the Raman peak caused by the vibration mode of edge-sharing (ES) of the $GeSe_{4/2}$ tetrahedral appears near 215 cm^{-1} [24,25]. The characteristic peaks of the homopolar bond Ge-Ge in the ethane-like $Se_2Ge{=}GeSe_2$ structure unit appear around 175 cm^{-1} and 300 cm^{-1}, respectively [23, 26-28]. For chalcogenide glasses As_xSe_{1-x}, the vibration peaks of $AsSe_{3/2}$ pyramidal units appear at 230 cm^{-1} and 268 cm^{-1} [29-31]. The vibration peak at around 247 cm^{-1} is ascribed to the homopolar bond As-As of the As_4Se_4 structural unit [32]. However, due to the vibration modes of the ternary Ge-As-Se glass are overlapping each other, and the Ge, As and Se atom are very close to each other in the periodic table of elements (atomic radius and mass are similar), therefore, it is difficult to distinguish each structural unit one by one in the Raman spectra.

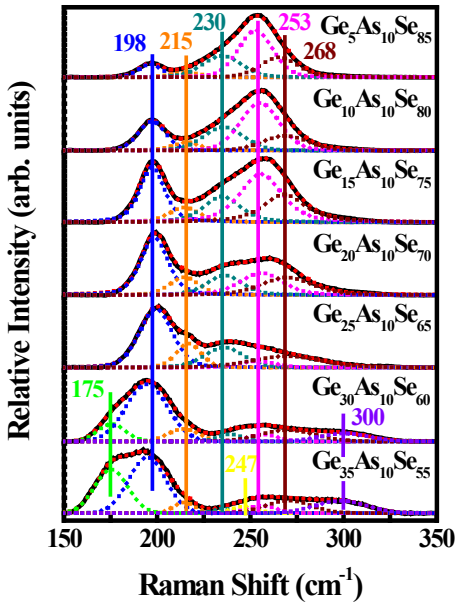

Fig. 3. Raman spectra of $Ge_xAs_{10}Se_{90-x}$ glasses and their decompositions.

We decompose the measured Raman spectra according to the Raman characteristic peaks corresponding to the above structural units, and the results are shown in the Fig. 3. Based on the simulation results of Raman spectra, we calculated the relative ratio of the integrated area of each decomposed peak to that of the whole area of Raman spectra, from which the variation trend of each structure with the glasses chemical composition and MCN and the results were plotted in Fig. 4. We observe that the maximum relative number of $GeSe_{4/2}$ (CS) and (ES) structural units was founded in the $Ge_{25}As_{10}Se_{65}$ glasses. For heteropolar bond As-Se, the increase of the Ge concentration has almost no influence before the glass composition reaches chemically stoichiometric. Once the glass composition exceeds the chemically stoichiometric, the heteropolar bond As-Se decrease with increasing Ge concentration. The homopolar bonds (Ge-Ge and As-As) almost do not exist in the low Ge concentration glasses, however, they appear when the glass composition exceeds the chemically stoichiometric, and their quantity increases with the increase of Ge concentration. For homopolar Se-Se bonds, its quantity gradually decreases with the increase of Ge concentration, and finally disappears in the $Ge_{25}A_{10}Se_{65}$ glasses.

The above evolution is basically consistent with the expected results of ternary Ge-As-Se glass. Starting from glass with low Ge concentration, Se-rich glass has desirable $GeSe_{4/2}$ and $AsSe_{3/2}$ structural units, and $GeSe_{4/2}$ (CS) and (ES) units with the increase of Ge concentration, while the relative number of $AsSe_{3/2}$ structural units remains constant until the glass composition reaches the chemically stoichiometric, all Se atom in the glass network structure bond with Ge and As atoms. However, when the glass composition exceeds the chemically stoichiometric, the Ge-Se-Se glasses becomes Se-poor, so there are no more Se atoms to be bonded with Ge or As, and only Ge-Ge and As-As homopolar bonds are formed for the extra Ge and As. This can be reflected in the increase of the relative intensity of the corresponding characteristic peak in Fig. 3. At the same time, by comparing the evolution of each chemical bond in Fig. 4, it can also be seen that with the increase of Ge content, the homopolar Ge-Ge bond is formed before As-As bond.

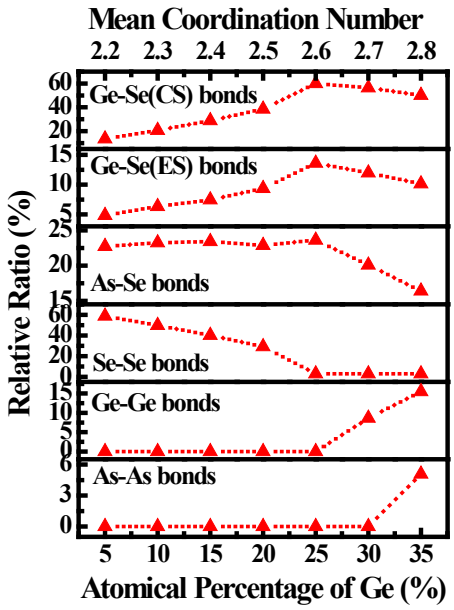

Fig. 4. Relative number of the bonds derived from the simulation of each Raman spectra.

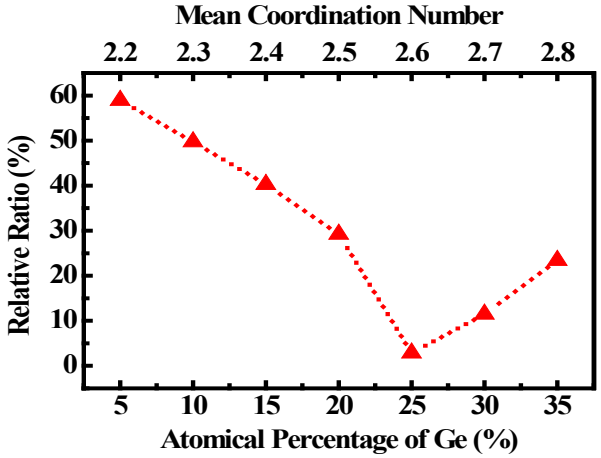

Fig. 5. Relative ratio of the homopolar bonds derived from the decomposed Raman spectra.

Fig. 5 shows the variation trend of all homopolar bonds (Ge-Ge, As-As and Se-Se) with chemical composition and MCN. It can be found that whether with the increase of Ge

concentration or MCN of $Ge_xAs_{10}Se_{90-x}$ glasses, the total number of homopolar bonds in chalcogenide glasses shows the same change trend, that is, first decreases and then increases. The minimum value was found at MCN=2.60, and the corresponding chemically stoichiometric glasses $Ge_{25}As_{10}Se_{65}$. Therefore, it can be inferred that the number of homopolar bonds is minimum and the order degree of the glass network structure is higher when the glass composition is in the chemically stoichiometric. Based on this, the variation of E_g of glass with composition can also be well explained. In amorphous materials, the existence of homopolar bonds will lead to the formation of band tails, and the more the number of them, the narrower the E_g of the glass [33-35].

4. Conclusions

A series of $Ge_xAs_{10}Se_{90-x}$ glasses were prepared to study the influence of chemical composition and mean coordination number on its structure and physical properties. On the one hand, the physical properties of the glasses were tested and analyzed. It was found that with the increase of Ge content, the refractive index of glass decreases initially and then increases, the E_g increases and then decreases, the transition behavior occurs in the glass composition satisfying the chemically stoichiometric composition. On the other hand, through the decomposition of Raman spectra, we found that the number of homopolar bonds (Ge-Ge, As-As, and Se-Se) is the smallest in the chalcogenide glass $Ge_{25}As_{10}Se_{65}$ with chemically stoichiometric composition. A clear correlation was found between the physical properties and the structure of the glasses. In other words, as the number of homopolar bonds decreases, the refractive index of the chalcogenide glasses becomes smaller and the E_g of the chalcogenide glasses becomes larger. Therefore, it can be concluded that the chemical composition plays a dominant role in determining the structure and properties of $Ge_xAs_{10}Se_{90-x}$ chalcogenide glasses.

Acknowledgements

This research is supported by the National Natural Science Foundation of China (No. 62004067), the Research Foundation of Education Bureau of Hunan Province (No. 21B0620) and the Teaching reform Foundation of Hunan University of Arts and Sciences (No. JGYB2049).

References

[1] R. P. Wang, Amorphous Chalcogenides: Advances and Applications, Pan Stanford Publisher, Singapore, 101-128 (2014); https://doi.org/10.1201/b15599

[2] L. Niu, Y. M. Chen, X. Shen, T. F Xu, Chinese Physics B 29(8), 087803 (2020); https://doi.org/10.1088/1674-1056/aba273

[3] S. W. Xu, X. N. Yang, J. H. Yang, R. X. Wang, X. Q. Su, Chalcogenide Letters 18(6), 277 (2021).

[4] J.Kang, R. K. Kotnala, S. K. Tripathi, Chalcogenide Letters 17(12), 631 (2020).

[5] A. P. Yang, M. Y. Sun, H. Ren, H. X. Lin, X. Feng, Z. Y. Yang, Journal of Luminescence 237, 118169 (2021); https://doi.org/10.1016/j.jlumin.2021.118169

[6] B. J. Eggleton, B. Luther-Davies, K. Richardson, Nature Photonics 5(3), 141 (2011); https://doi.org/10.1038/nphoton.2011.309

[7] Z. M. Zhao, B. Wu, X. S. Wang, Z. H. Pan, Z. J. Liu, P. Q. Zhang, X. Shen, Q. H. Nie, S. X. Dai, R. P. Wang, Laser & Photonics Reviews 11(2), 1700005 (2017); https://doi.org/10.1002/lpor.201700005

[8] Y. Yu, X. Gai, P. Ma, K. Vu, Z. Y. Yang, R. P. Wang, D. Y. Choi, S. Madden, B. Luther-Davies, Optics Letters 41(5), 958 (2016); https://doi.org/10.1364/OL.41.000958

[9] J. Ren, X. S. Lu, C. G. Lin, R. K. Jain, Optics Express 28(15), 21522 (2020); https://doi.org/10.1364/OE.395402

[10] X. Gai, T. Han, A. Prasad, S. Madden, D. Y. Choi, R. P. Wang, D. Bulla, B. Luther-Davies, Optics Express 18(25), 26635 (2010); https://doi.org/10.1364/OE.18.026635

[11] A. Dahshan, H. H. Hegazy, K. A. Aly, Chalcogenide Letters 16(10), 499 (2019).

[12] H. T. Lin, Y. Song, Y Z. Huang, D. Kita, S. Deckoff-Jones, K. Q. Wang, L. Li, J. Y. Li, H. Y. Zheng, Z. Q. Luo, H. Z. Wang, S. Novak, A. Yadav, C. C. Huang, R. J. Shiue, D. Englund, T. Gu, D. Hewak, K. Richardson, J. Kong, J. J. Hu, Nature Photonics 11, 798 (2017); https://doi.org/10.1038/s41566-017-0033-z

[13] J. C. Phillips, Journal of Non-Crystalline Solids 34(2), 153 (1979); https://doi.org/10.1016/0022-3093(79)90033-4

[14] M. F. Thorpe, Journal of Non-Crystalline. Solids 57(3), 355 (1983); https://doi.org/10.1016/0022-3093(83)90424-6

[15] K. Tanaka, Physical Review B 39(2), 1270 (1989); https://doi.org/10.1103/PhysRevB.39.1270

[16] P. Toronc, M. Bensoussan, A. B. Renac, Physical Review B 8(12), 5947 (1973); https://doi.org/10.1103/PhysRevB.8.5947

[17] T. Wang, O. Gulbiten, R. P. Wang, Z. Y. Yang, A. Smith, B. Luther-Davies, P. Lucas, The Journal of Physical Chemistry B 118(5), 1436 (2014); https://doi.org/10.1021/jp412226w

[18] Y. Yang, Z. Y. Yang, P. Lucas, Y. W. Wang, Z. J. Yang, A. P. Yang, B. Zhang, H. Z. Tao, Journal of Non-Crystalline Solids 440, 38 (2016); https://doi.org/10.1016/j.jnoncrysol.2016.03.003

[19] D. C. Kaseman, I. Hung, Z. H. Gan, B. Aitken, S. Currie, S. Sen, The Journal of Physical Chemistry B 118(8), 2284 (2014); https://doi.org/10.1021/jp412451h

[20] I. P. Kotsalas, D. Papadimitriou, C. Raptis, M. Vlcek, M. Frumar, Journal of Non-Crystalline Solids 226(1-2), 85 (1998); https://doi.org/10.1016/S0022-3093(97)00493-6

[21] G. Yang, B. Bureau, T. Rouxel, Y. Gueguen, O. Gulbiten, C. Roiland, E. Soignard, J. L. Yarger, J. Troles, J. C. Sangleboeuf, P. Lucas, Physical Review B 82(19), 195206 (2010); https://doi.org/10.1103/PhysRevB.82.195206

[22] W. H. Wei, R. P. Wang, X. Shen, L. Fang, B. Luther-Davies, The Journal of Physical Chemistry C 117(32),16571 (2013); https://doi.org/10.1021/jp404001h

[23] K. Jackson, A. Briley, S. Grossman, D. V. Porezag, M. R. Pederson, Physical Review B 60(22), R14985 (1999); https://doi.org/10.1103/PhysRevB.60.R14985

[24] Z. Cernosek, E. Cernoskova, R. Todorov, J. Holubova, Journal of Solid State Chemistry 291, 121599 (2020); https://doi.org/10.1016/j.jssc.2020.121599

[25] K. Shportko, L. Revutska, O. Paiuk, J. Baran, A. Stronski, A. Gubanova, E. Venger, Optical Materials 73, 489 (2017); https://doi.org/10.1016/j.optmat.2017.08.042

[26] R. P. Wang, A. Smith, A. Prasad, D. Y. Choi, B. Luther-Davies, Journal of Applied Physics 106(4), 043520 (2009); https://doi.org/10.1063/1.3204951

[27] R. P. Wang, D. Y. Choi, A. V. Rode, S. J. Madden, B. Luther-Davies, Journal of Applied Physics 101(11), 113517 (2007); https://doi.org/10.1063/1.2737785

[28] M. Reinfelde, M. Mitkova, T. Nichol, Z.G. Ivanova, J. Teteris, Chalcogenide Letters 15(1), 35

(2018).

[29] S. W. Xu, R. P. Wang, Z. Y. Yang, L. Wang, B. Luther-Davies, Applied Physics Express 8(1), 015504 (2015); https://doi.org/10.7567/APEX.8.015504

[30] S. W. Xu, R. P. Wang, Z. Y. Yang, L. Wang, B. Luther-Davies, Chinese Physics B 25(5), 057105 (2016); https://doi.org/10.1088/1674-1056/25/5/057105

[31] R. I. Alekberov, S. I. Mekhtiyeva, A. I. Isayev, M. Fabian, Q. Tian, L. Almasy, Chalcogenide Letters 14(3), 79 (2017).

[32] B. Yuan, H. Chen, S. Sen, The Journal of Physical Chemistry B 126(4), 946 (2022); https://doi.org/10.1021/acs.jpcb.1c08836

[33] S. Mamedov, D. G. Georgiev, T. Qu, P. Boolchand, Journal of Physics: Condensed Matter 15(31), S2397 (2003); https://doi.org/10.1088/0953-8984/15/31/315

[34] K. Hachiya, Journal of Non-Crystalline Solids 321(3), 217 (2003); https://doi.org/10.1016/S0022-3093(03)00238-2

[35] K. Tanaka, K. Shimakawa, Amorphous Chalcogenide Semiconductors and Related Materials, Springer International Publishing, New York, 110-121 (2011); https://doi.org/10.1007/978-1-4419-9510-0_5